Macromolecules

pubs.acs.org/Macromolecules Article

Organocatalyzed Synthesis and Degradation of Functionalized Poly(4-allyloxymethyl-β-propiolactone)s

Yeji Yu, Minseong Kim, Gue Seon Lee, Hyo Won Lee, Jeung Gon Kim, and Byeong-Su Kim*

Cite This: *Macromolecules* 2021, 54, 10903−10913 Read Online

ACCESS | Metrics & More | Article Recommendations | Supporting Information

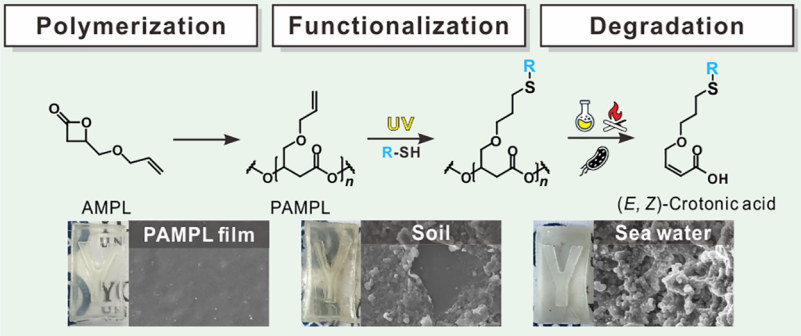

ABSTRACT: The chemical synthesis of degradable poly(β-hydroxyalkanoate) (PHA) produced by microorganisms allows the control of the solubility, crystallinity, hydrophobicity, degradability, thermal, and mechanical properties by introducing functionality on the side chain. Herein, we synthesized a PHA derivative containing a pendant allyl group via the anionic ring-opening polymerization of a 4-allyloxymethyl-β-propiolactone (AMPL) monomer, which was prepared via the carbonylation of allyl glycidyl ether. The AMPL monomer was subjected to various organocatalysts in bulk to yield poly(4-allyloxymethyl-β-propiolactone) (PAMPL) with controllable molecular weight and dispersity. The prepared PAMPL polymers were characterized via ^{1}H and ^{13}C NMR, gel permeation chromatography (GPC), differential scanning calorimetry (DSC), and matrix-assisted laser desorption/ionization-time-of-flight (MALDI-TOF) analyses. A photoactivated thiol−ene reaction allowed the postpolymerization modification of PAMPLs with varying substituents. Functionalized PAMPL polymers degraded under chemical and thermal conditions, and importantly, cross-linked PAMPL films degraded during exposure to soil and seawater under a wide range of degradation kinetics. This study provides the future potentials of the chemically synthesized and functionalized PHA for replacing conventional petroleum-derived polymers.

INTRODUCTION

Due to their advantageous properties, including low cost, light weight, versatile processing, and good mechanical properties, petroleum-based plastics have contributed to our daily life. However, the cumulative impact of nondegradable plastics is causing critical issues due to the limited fossil fuel resources and environmental burden with severe accumulation of plastics in nature, which thus has prompted the search for alternative sources.[1−3]

To replace the existing petroleum-based polymers, biobased and biodegradable polymers are suggested, including plant-based polymers (e.g., starch and cellulose), biomonomer-based polymers (e.g., polylactic acid and biopolyethylene), and extracted biopolymers [e.g., poly(β-hydroxyalkanoate) (PHA)]; compared to petroleum-based polymers, they afford significantly lower carbon dioxide emission and energy requirements.[4−6] Among them, PHAs are well-known aliphatic polyesters that can be produced using microorganisms, which accumulate as intracellular granules for energy-storage purposes.[7,8] Moreover, only PHAs are completely compostable and marine biodegradable,[9] providing a potential solution to prevent air, soil, and marine pollution. Therefore, PHAs afford a wide range of potential applications, such as in the biomedical, food packaging, agriculture, and energy fields.[10] However, compared to commercial petroleum-based polymers, the widespread applications of PHAs are limited by their high production costs associated with additional nutrients and energy costs as well as their low production efficiency due to extraction with organic solvents.[9,11,12]

Therefore, chemical syntheses such as ring-opening polymerization,[13,14] directive carbonylative polymeriza-

Received: September 5, 2021
Revised: October 30, 2021
Published: November 16, 2021

https://doi.org/10.1021/acs.macromol.1c01879
Macromolecules 2021, 54, 10903−10913

Scheme 1. Synthesis and Degradation of Functionalized Poly(4-allyloxymethyl-β-propiolactone) (PAMPL) with Varying Pendant Groups (R_1−R_4) and a Cross-Linked Film

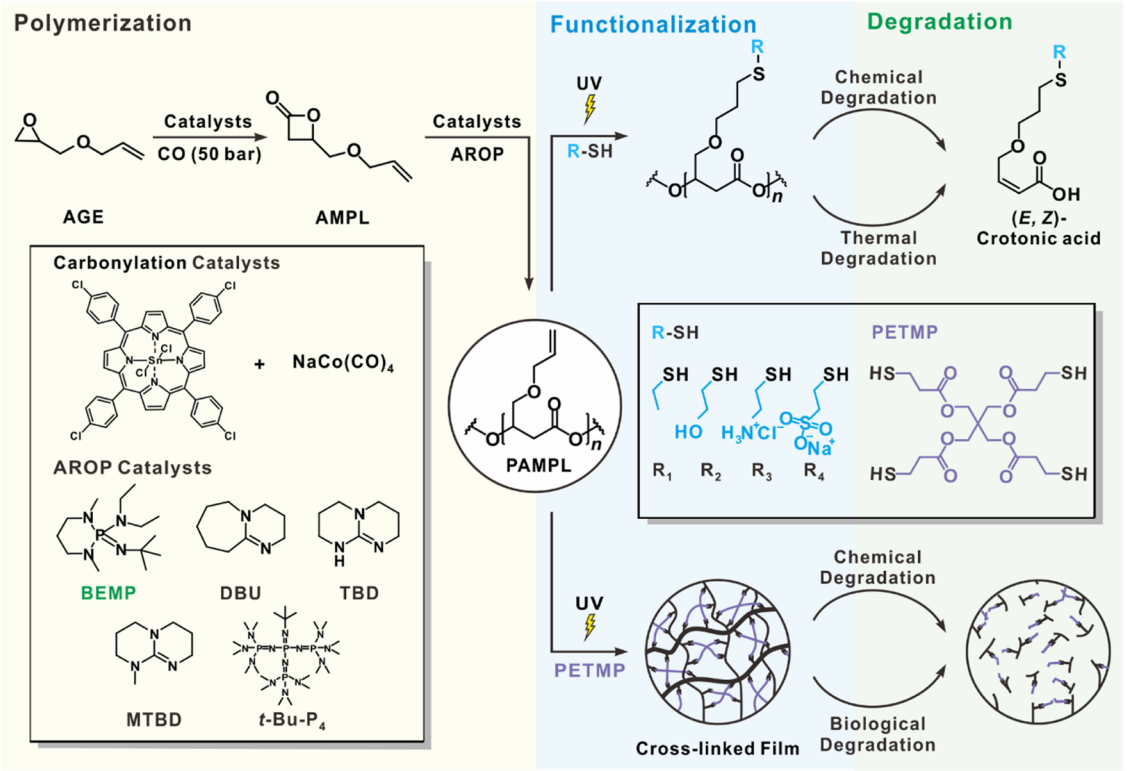

tion,[15−17] and step-growth polymerization have been investigated as alternative routes to synthesize PHAs.[18−20] Among these approaches, the controlled ring-opening polymerization of β-lactone allows the production of high-molecular-weight PHAs (M_n > 100 000) with excellent reactivity and productivity.[13,21,22] This polymerization process has been traditionally mediated by highly effective metal-based salts or discrete metal complexes, enabling to achieve a high stereochemical control of the microstructure or alternation with chiral racemic β-substituted β-lactones.[23−27] More recently, metal-free organocatalysts have been employed as an effective approach for the ring-opening polymerization of β-lactones under mild conditions with unique advantages, such as cost effectiveness, high chemical tunability, high stability, and high performance.[13,28−30]

To date, most previous studies have utilized β-butyrolactone as a representative monomer for the chemical synthesis of polyhydroxybutyrate.[31−33] However, these isotactic polyhydroxybutyrates containing methyl substituents often suffer from poor thermal and mechanical properties, limiting their widespread uses.[34,35] The incorporation of other polymers into polyhydroxybutyrates can alleviate these issues; however, they will lose their biodegradable functionality and become less environmentally sustainable.

To tailor the properties of PHAs, β-lactone monomers with various substituents can be prepared through nucleophile-catalyzed cycloadditions of ketenes with aldehydes,[36] lactonization via the activation of the carboxylic acid with various coupling agents,[37] and the carbonylation of various epoxides.[38−41] Especially, β-lactones containing an allyl functional group can offer well-defined polymers with tunable properties through postpolymerization modification (PPM), which can provide various functional groups across a single polymer.[42−47] Therefore, the development of a monomer for the controlled synthesis of PHA with tunable properties is highly desirable.

Herein, we propose a simple chemical synthetic strategy for producing biodegradable poly(4-allyloxymethyl-β-propiolactone) (PAMPL) containing a pendant allyl group via the anionic ring-opening polymerization (AROP) of 4-allyloxymethyl-β-propiolactone (AMPL) using various organocatalysts in bulk (Scheme 1). The AMPL monomer, a derivative of β-lactone, was prepared via the carbonylation of allyl glycidyl ether (AGE) in a highly specific manner. Notably, the PAMPL properties were highly controlled via PPM with various thiol-bearing molecules through the photoactivated thiol−ene reaction. An additional benefit of this study is to investigate the biodegradable properties under various conditions. A transparent cross-linked PAMPL film was prepared and degraded in chemical, soil, and marine conditions, indicating the potential applications of the chemically synthesized PAMPL to replace the conventional petroleum-derived polymers.

EXPERIMENTAL SECTION

Materials. (*R*,*S*)-Allyl glycidyl ether (AGE, 99%), 1,5,7-triazabicyclo[4.4.0]dec-5-ene (TBD, 98%), 2-*tert*-butylimino-2-diethylamino-1,3-dimethylperhydro-1,3,2-diazaphosphorine (BEMP, 98%), 7-methyl-1,5,7-triazabicyclo[4.4.0]dec-5-ene (MTBD, 98%), *t*-BuP_4 phosphazene base solution (0.80 M in hexane), 2,2-dimethoxy-2-phenylacetophenone (DMPA, 99%), pentaerythritol tetrakis(3-mercaptopropionate) (PETMP, 95%), ethanethiol, sodium 2-mercaptoethanesulfonate (98%), and cysteamine hydrochloride (98%) were purchased from Sigma-Aldrich. 1,8-Diazabicyclo[5.4.0]-undec-7-ene (DBU, 98%) was purchased from the Tokyo Chemical Industry. 2-Mercaptoethanol (98%) was purchased from Alfa Aesar, and all reagents were used as received unless otherwise noted. The deuterated NMR solvents $CDCl_3$, MeOD, and D_2O were purchased

https://doi.org/10.1021/acs.macromol.1c01879
Macromolecules 2021, 54, 10903−10913

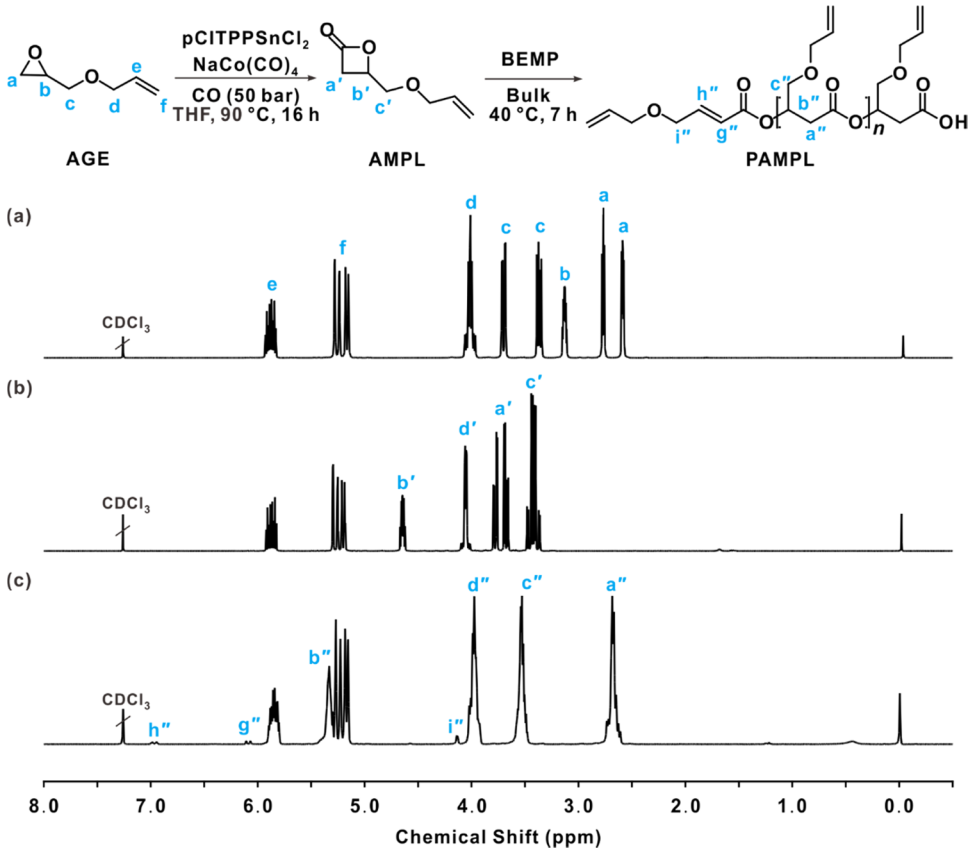

Figure 1. Representative synthetic routes with the corresponding ^{1}H NMR spectra of (a) AGE, (b) AMPL, and (c) PAMPL (entry 2 in Table 1). See the Experimental section for details.

from Cambridge Isotope Laboratories. AMPL was synthesized according to the procedure reported in the literature.[38] AGE and AMPL were degassed through several freeze−pump−thaw cycles followed by purification with CaH_2 via cryodistillation.

Characterizations. ^{1}H, ^{13}C, correlation spectroscopy (COSY), and heteronuclear single quantum correlation (HSQC) NMR spectra were recorded on a Bruker 400 MHz spectrometer at room temperature. The number-averaged (M_n) and weight-averaged molecular weights (M_w) and molecular weight distribution (M_w/M_n, $Đ$) were measured via gel permeation chromatography (GPC) using an Agilent 1200 series with tetrahydrofuran (THF) as an eluent at 25 °C at a flow rate of 1.00 mL min^{-1} using a refractive index (RI) detector. All calibrations were performed using polystyrene (PS) standards. Fourier transform infrared (FTIR) spectra were recorded on an Agilent Cary 630 FTIR spectrometer with an attenuated total reflection (ATR) module. Differential scanning calorimetry (DSC) (Q200 model, TA Instruments) was performed under a nitrogen atmosphere from −80 to 200 °C with a heating rate of 10 °C min^{-1}. Matrix-assisted laser desorption and ionization-time-of-flight (MALDI-TOF) mass spectrometry (MS) was performed on a Bruker Autoflex Max with α-cyano-4-hydroxycinnamic acid as the matrix. The films' mechanical properties were measured using a universal testing machine (UTM, Instron 5943). The cross-linked films (0.50 mm in thickness) were cut in a dumbbell shape (24 × 16 × 0.50 mm^3) using a cutting die (ASTM D412). The cross-head speed was 1 mm min^{-1}, and the specimen was tested more than three times. The surface morphology of the PAMPL films was analyzed via field-emission scanning electron microscopy (FE-SEM, JEOL, IT-500HR).

Synthesis of the AMPL Monomer. In a glovebox, a stainless-steel reactor was placed with *p*-ClTPPSnCl$_2$ (113 mg, 0.12 mmol), NaCo(CO$_4$) (47 mg, 0.24 mmol), and THF (20 mL), and then, AGE (4.71 mL, 40 mmol) was added. The reactor was properly sealed and removed from the glovebox. Thereafter, it was purged thrice with CO gas and slowly pressurized to 50 bar pressure, and stirred at 90 °C. After 16 h, the reactor was cooled at room temperature. Excess CO gas was slowly vented. The mixture was filtered through a short column packed with silica gel using diethyl ether. AMPLs were further purified via flash column chromatography using hexane/ethyl acetate (4:1, v/v) as an eluent and distillation, affording AMPL as a colorless liquid in a 90% yield. ^{1}H NMR (400 MHz, $CDCl_3$): δ 5.94−5.79 (m, 1H), 5.27 (dq, J = 17.3, 1.6 Hz, 1H), 5.22−5.16 (m, 1H), 4.65 (dtd, J = 5.8, 4.5, 3.0 Hz, 1H), 4.07−4.03 (m, 2H), 3.72 (ddd, J = 16.2, 11.7, 3.7 Hz, 2H), 3.42 (dd, J = 11.3, 5.2 Hz, 2H). ^{13}C NMR (101 MHz, $CDCl_3$): δ 167.75, 134.05, 117.75, 72.68, 69.47, 69.36, 39.74.

General Synthesis of PAMPL. In a glovebox, AMPL (1.00 g, 7.04 mmol) and BEMP (40.80 μL, 0.14 mmol) were added into a flask, which was flame dried under a vacuum. Then, the mixture was stirred in an oil bath at 40 °C. The reaction was monitored via ^{1}H NMR to determine the residual AMPL monomer signals during the progress of the reaction. After the reaction was completed, the polymerization was quenched thrice for 2 h by ion-exchange resin (Amberlite IR-120(H)) treatment to remove the organocatalysts used. To remove any monomer and other impurities, precipitation was performed twice in pentane. The precipitated PAMPL polymer was dried under a high vacuum. M_n and $Đ$ values were determined via ^{1}H NMR and GPC analyses, respectively. ^{1}H NMR (400 MHz, $CDCl_3$): δ 7.02−6.92 (m, 1H), 6.14−6.05 (m, 1H), 5.94−5.76 (m, 52H), 5.39−5.31 (m, 49H), 5.29−5.11 (m, 107H), 4.13 (dd, J = 4.2, 2.0 Hz, 2H), 4.08−3.89 (m, 111H), 3.63−3.46 (m, 107H), 2.76−2.59 (m, 106H). ^{13}C NMR (101 MHz, $CDCl_3$): δ 172.06, 169.55, 165.45, 145.24, 134.42, 120.91, 117.42, 72.24, 70.16, 69.50, 68.63, 35.88. GPC (THF, PS standard): M_n = 6520 g mol^{-1} and $Đ$ = 1.10.

General Procedure for the Thiol−Ene Reaction. Briefly, as a representative example, the reaction with cysteamine hydrochloride for the preparation of P_3 is described herein. The thiol−ene reaction between the PAMPL polymer (150 mg, 0.22 mmol) and cysteamine hydrochloride (360 mg, 3.17 mmol; 3.0 equiv for each "ene" moiety) using DMPA (13.60 mg, 0.05 mmol; 0.05 equiv for each ene moiety)

https://doi.org/10.1021/acs.macromol.1c01879
Macromolecules 2021, 54, 10903−10913

Table 1. Characterizations of the Synthesized Poly(4-allyloxymethyl-β-propiolactone) (PAMPL)

entry	catalyst	AMPL (equiv)	temp. (°C)	time (h)	conv.[a] (%)	$M_{n,th}$[b] (g mol^{-1})	$M_{n,NMR}$[c] (g mol^{-1})	$M_{n,GPC}$[d] (g mol^{-1})	DP[d]	$Đ$[d]
1	BEMP	50	60	6	>99	7110	4260	4530	32	1.17
2	BEMP	50	40	7	92	6540	5690	6520	46	1.10
3	BEMP	200	60	72	96	27 290	8960	11 930	84	1.97
4	BEMP	200	40	72	80	22 740	15 640	16 870	118	1.15
5	*t*-BuP$_4$	50	60	6	>99	7110	2700	1290	9	1.44
6	DBU	50	60	24	81	5760	4990	2830	20	1.17
7	TBD	50	60	24	87	6180	4830	4450	31	1.22
8	MTBD	50	60	24	28	1990	3550	3490	25	1.11

[a]AMPL conversion as determined by the ^{1}H NMR spectra of the crude reaction mixture. [b]Theoretical molar mass calculated from the relation: AMPL (equiv) × conv.$_{AMPL}$ × M_{AMPL} (including initiator and end group moieties), with M_{AMPL} = 142.15 g mol^{-1}. [c]Determined by the ^{1}H NMR spectra of the isolated polymer in $CDCl_3$. [d]Determined by GPC in THF using the RI signal and a PS standard.

as a photoinitiator under UV irradiation (λ = 365 nm) for 12 h was performed according to the literature.[46] The reaction was monitored via ^{1}H NMR to determine the complete disappearance of the alkene peaks at 5.22 and 5.91 ppm. The reaction mixture was dialyzed against dimethyl sulfoxide (DMSO) and then water (MWCO 1 kDa dialysis membrane, Fisher Scientific) for 12 h; thereafter, the purified P_3 was concentrated under vacuum to yield a yellow polymer. ^{1}H NMR (400 MHz, D_2O): δ 5.39 (s, 1H), 3.64 (d, J = 4.6 Hz, 3H), 3.60 (s, 1H), 3.22 (d, J = 2.9 Hz, 2H), 2.85 (d, J = 2.9 Hz, 2H), 2.78 (d, J = 3.1 Hz, 2H), 2.64 (t, J = 6.9 Hz, 2H), 1.91−1.80 (m, 2H).

Preparation of the Photopolymerized PAMPL Film. The polymeric PAMPL film was produced by drop-casting the polymeric mixture (homogeneously mixing PAMPL (250 mg, 1.76 mmol), PETMP (0.50 mL, 1.32 mmol; 3.00 equiv for each ene moiety), and DMPA (22.5 mg, 0.09 mmol; 0.05 equiv for each ene moiety) in dried THF) on the glass and Y-shaped silicon mold while evaporating the solvent under the stream of nitrogen and UV light exposure (λ = 365 nm) for 15 min. The reaction was monitored via FTIR to determine the complete disappearance of the alkene peaks at 1645 cm^{-1}.

General Procedure for the Chemical Degradation of Functionalized PAMPL in BEMP. BEMP (81.2 μL, 0.28 mmol) and 153 mg of the P_1 (0.02 mmol) solution sample were added to 2.80 mL of dichloromethane (DCM). The reaction mixture was stirred in an oil bath at 40 °C. The postdegradation products were analyzed using ^{1}H NMR, GPC, and FTIR.

General Procedure for the Thermal Degradation of the Functionalized PAMPL. P_1 was thermally treated in an oil bath at 230 °C in ambient conditions. The postdegradation products were analyzed using ^{1}H NMR, GPC, and FTIR.

Chemical Degradation of the Polymer Films. The prepared cross-linked PAMPL films were individually weighed. Each piece of the film was placed in a screw-capped specimen tube. Degradation was performed at 40 °C in 0.10 M BEMP in DCM, 0.10 M NaOH, and 0.10 M HCl solution. Then, the films were washed with distilled water and dried in a vacuum oven at room temperature for 24 h. The degradation rate was determined by periodic recovery to check the weight loss.

Biological Degradation of Polymer Films in Soil and Seawater. The prepared cross-linked PAMPL films were individually weighed. Three films (10 × 20 mm^2, 60−70 mm in thickness) were buried in a 900 mL crystallizing dish (Duran) filled with 300 g of the compost mixture, a commercial garden soil/compost mixture (5:5, w/w), to facilitate airflow with the water content maintained at 50% (v/w), and were incubated at 50 °C for 60 days.[48] Additionally, the films were placed into 20 mL vials filled with 15 mL of seawater (Pohang, the East Sea of Korea). The films were washed with distilled water and dried in a vacuum oven at room temperature for 24 h. The degradation rate was determined by periodic recovery to check the weight loss.

RESULTS AND DISCUSSION

Synthesis and Characterization of the AMPL Monomer. The AMPL monomer was synthesized via carbonylation of AGE with CO (50 bar) using Sn(IV) porphyrins with a tetracarbonyl cobaltate catalyst, exhibiting exclusive selectivity to AMPL without any side products or double carbonylation, as developed in our previous study.[38] Subsequently, AMPL was isolated as a transparent liquid in a 90% yield. ^{1}H, ^{13}C, COSY, and HSQC NMR spectra verified the monomer structure (Figures 1a,b and S1−S3 in the Supporting Information). In the representative ^{1}H NMR spectra of AMPL, methylene protons in the α-position and methine protons adjacent to the allyloxymethyl group of the AMPL appeared at 3.75−3.82 and 4.62−4.69 ppm, respectively, indicating successful monomer synthesis.

Synthesis and Characterization of PAMPL. PAMPL was synthesized via the AROP of AMPL using various catalytic systems, including BEMP, DBU, TBD, MTBD, and *t*-BuP$_4$, as organocatalysts in bulk (Table 1). For AMPL, the monomer conversion was monitored via ^{1}H NMR spectroscopy by observing the reduction of methylene and methine peaks of the β-lactones (Figure 1b,c). Purified PAMPL was obtained after treatment with the ion-exchange resin to remove protonated organocatalysts and precipitated in pentane.[49]

Both BEMP and *t*-BuP$_4$, a highly basic and bulky organocatalyst, proved significantly more active than the other organocatalysts. Specifically, both BEMP and *t*-BuP$_4$ afforded the AROP of AMPL with a full conversion in 6 h at 60 °C (entry 1 and 5 in Table 1). In contrast, the AROP of DBU, TBD, and MTBD resulted in monomer conversions of 81, 87, and 28% in 24 h, respectively (entry 6−8 in Table 1), under identical reaction conditions. Interestingly, the polymer structures also differed depending on the type of organocatalyst used.[13,29] For example, both BEMP and *t*-BuP$_4$ acted as bases, whereas DBU, TBD, and MTBD displayed dual activity as bases and nucleophiles.

As shown in Figure 1c, the ^{1}H NMR spectra of PAMPL prepared using BEMP clearly display characteristic peaks corresponding to crotonate initiator protons (6.05−6.14 and 6.92−7.02 ppm) and methine and methylene protons of the polymeric backbone (5.31−5.39 and 2.61−2.74 ppm). Moreover, the MALDI-TOF mass spectrum of PAMPL demonstrated a single mass population with a constant interval of 142.15 g mol^{-1}, corresponding to the molecular weight of the AMPL monomer. The molecular weight of 1159.75 and 1176.25 g mol^{-1} corresponded to a homopolymer chain end-capped with an allyloxymethylcrotonate initiator (141.15 g mol^{-1}), six monomer units, carboxylic acid groups (143.15 g mol^{-1}), and Na^+ and K^+ as the counterions, respectively, suggesting a potential polymerization reaction mechanism (Figure S4).

https://doi.org/10.1021/acs.macromol.1c01879
Macromolecules 2021, 54, 10903−10913

Scheme 2. Proposed Mechanism for the Anionic Ring-Opening Polymerization of AMPL with BEMP as a Base

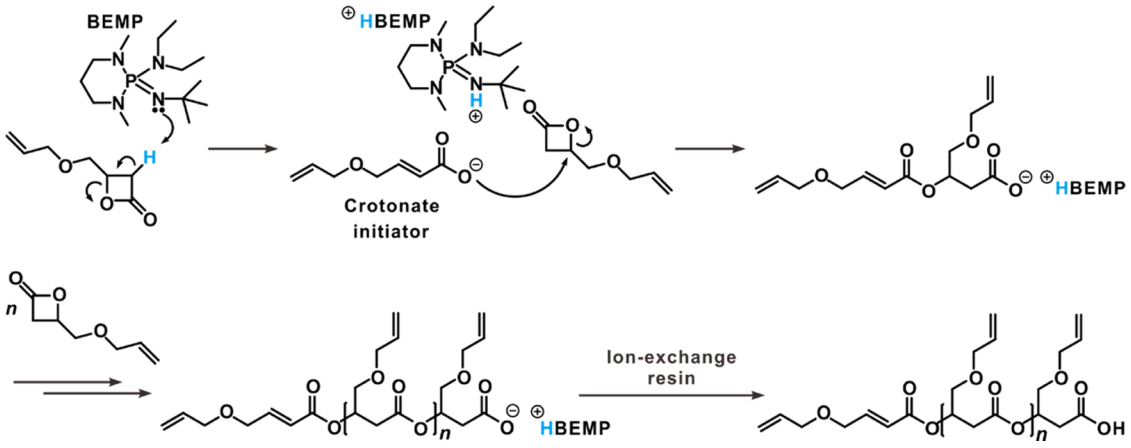

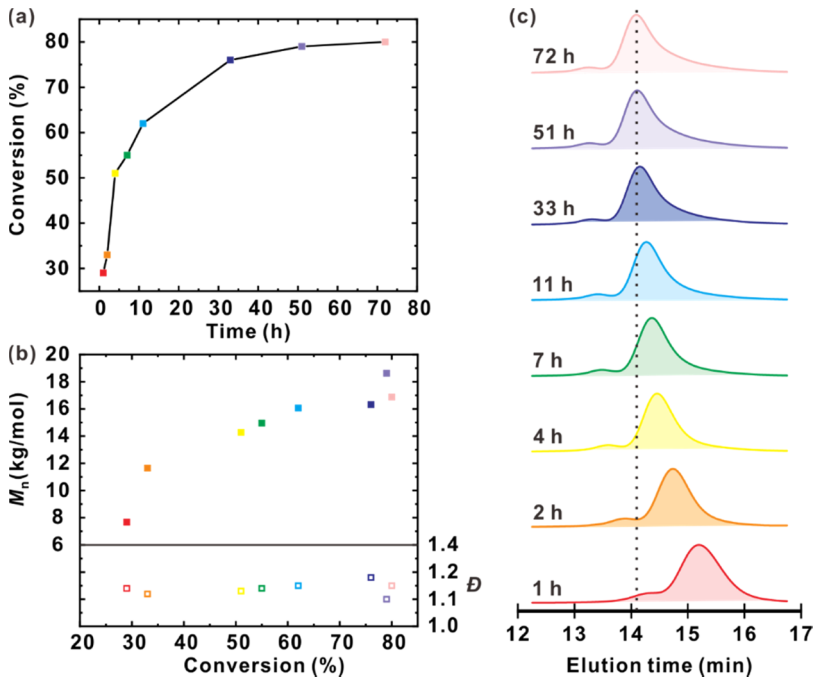

Figure 2. PAMPL polymerization kinetics. (a) Monomer conversion−time plot, (b) summary of molar mass (by ^{1}H NMR spectra) and dispersity (by GPC) with respect to the total monomer conversion, and (c) evolution of the normalized GPC over time (entry 4 in Table 1).

Although the polymerization results of *t*-BuP$_4$ were similar to those of BEMP (Figures S5 and S6), significant deviations were observed between the number-average molar mass ($M_{n,GPC}$) and theoretical molar mass ($M_{n,th}$) along with a broad dispersity ($Đ$) (entry 1 and 5 in Table 1). This is because the more sterically demanding *t*-BuP$_4$ protonated in the initiation process can be more readily separated from the growing carboxylate chain end compared to BEMP. Thus, a more active chain end can randomly abstract a proton from the α-position of an AMPL monomer, undergoing a chain-transfer reaction with the inter- and intrachain methylene groups.

Considering the NMR and MALDI-TOF results, we propose a polymerization mechanism with BEMP (Scheme 2). The highly basic and sterically demanding BEMP base generates a crotonate initiator by abstracting the α-hydrogen from the AMPL monomer. Subsequently, this weak nucleophilic crotonate attacks the β-carbon in the lactone ring with the alkyl-oxygen bond cleavage that proceeds with the AROP propagation, as similarly observed in the previous study of Kurcok et al.[50] The reaction between the BEMP and the monomer was further evaluated using ^{1}H NMR and ^{31}P NMR. A clear shift of peaks corresponding to BEMP upon protonation was observed compared to the free BEMP (Figure S7).

Unlike BEMP and *t*-BuP$_4$, DBU, TBD, and MTBD display dual activity as a base and a nucleophile, involving both alkyl-oxygen and acyl-oxygen cleavage of AMPL during the polymerization (Scheme S1). In the polymerization mediated by TBD, TBD-*N*-acyl-α,β-unsaturated species is first produced, followed by the propagation via acyl-oxygen cleavage.[13] The structures of PAMPL mediated by these organocatalysts were clearly identified via ^{1}H NMR and MALDI-TOF mass spectra. The ^{1}H NMR spectra exhibited PAMPL bearing both crotonate initiator and catalyst moieties, indicating a potential nucleophilic nature of the organocatalysts (Figures S8−S10).

Furthermore, the MALDI-TOF spectra of PAMPL mediated by DBU, TBD, and MTBD depicted two series of molecular ion peaks with a constant interval of 142.15 g mol^{-1} (Figures

https://doi.org/10.1021/acs.macromol.1c01879
Macromolecules 2021, 54, 10903−10913

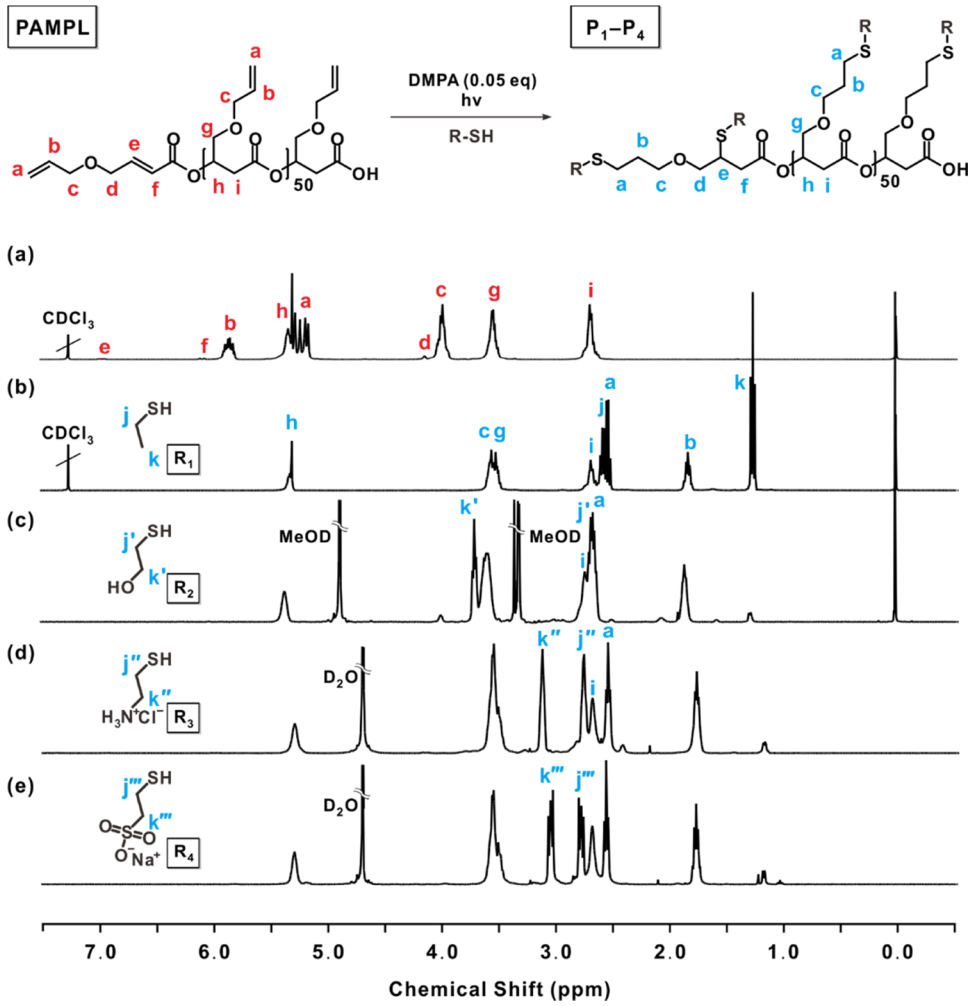

Figure 3. Postpolymerization modification of PAMPL via the thiol−ene reaction with different pendant groups (R_1−R_4). ^{1}H NMR spectra of (a) PAMPL, (b) P_1, (c) P_2, (d) P_3, and (e) P_4.

S11−S13). One series comprised a PAMPL chain end capped with a β-hydroxyester and organocatalyst moiety behaving as a nucleophile, while the other series comprised allyloxymethylcrotonate and a carboxylic acid chain end with Na^+ and K^+ as the counterions serving as a base. Although the three organocatalysts afford similar activities, compared to DBU (pK_b = −10.32) and TBD (pK_b = −12.03), MTBD (pK_b = −11.40) more predominantly behaved as a base than a nucleophile due to the steric hindrance of the methyl group, regardless of the pK_b values.

Among all organocatalysts investigated, BEMP, generating only a single type of PAMPL polymer by exclusively acting as a base, with a controlled molecular weight was found to be the most suitable catalyst. However, the theoretical and experimental molar mass of PAMPL mediated by BEMP at 60 °C slightly differed possibly due to the chain-transfer reactions (entry 1 in Table 1). Thus, the reaction temperature was further optimized at 40 °C, yielding a better match for the theoretical molecular weight of the PAMPL polymer, albeit with a slightly lower polymerization rate (entry 2 in Table 1). This indicates that the higher the reaction temperature, the more chain-transfer reactions involving monomers can occur either intra- or intermolecularly (Figure S14). The prepared PAMPL polymers were characterized via ^{1}H, ^{13}C, COSY, and HSQC NMR spectra (Figures 1c and S15−S17). The prepared PAMPL polymers exhibited a narrow dispersity ($Đ$ = 1.10), as confirmed by GPC ($M_{n,GPC}$) (Table 1).

To determine the controlled polymerization using the BEMP catalyst, the PAMPL polymerization kinetics was examined via ^{1}H NMR spectroscopy, and the total monomer conversion was determined as a function of reaction time (Figure 2a). At 40 °C, the monomer conversion increased with the polymerization time, reaching 80% in 72 h (entry 4 in Table 1). The linear increase in the molar mass ($M_{n,GPC}$) and a relatively low $Đ$ after the monomer conversion indicate that the reaction was well controlled (Figure 2b). Figure 2c shows the GPC overlay; the molar mass distribution of PAMPL shifts to lower elution over time, indicating the chain growth during the polymerization. The shoulder peak observed in GPC traces is possibly originated from the adventitious water.

PPM of PAMPL Via a Thiol−Ene Reaction. After the successful polymerization of PAMPL, the PPM of the pendant allyl groups was performed via a photoinitiated thiol−ene reaction. In the presence of the DMPA photoinitiator, the pendant allyl groups of PAMPL were efficiently converted into other functional moieties using four different thiol-based molecules, including ethanethiol (R_1), 2-mercaptoethanol (R_2), cysteamine hydrochloride (R_3), and sodium 2-mercaptoethanesulfonate (R_4), leading to the synthesis of the respective modified polymers of P_1−P_4 (Figure 3).

https://doi.org/10.1021/acs.macromol.1c01879
Macromolecules 2021, 54, 10903−10913

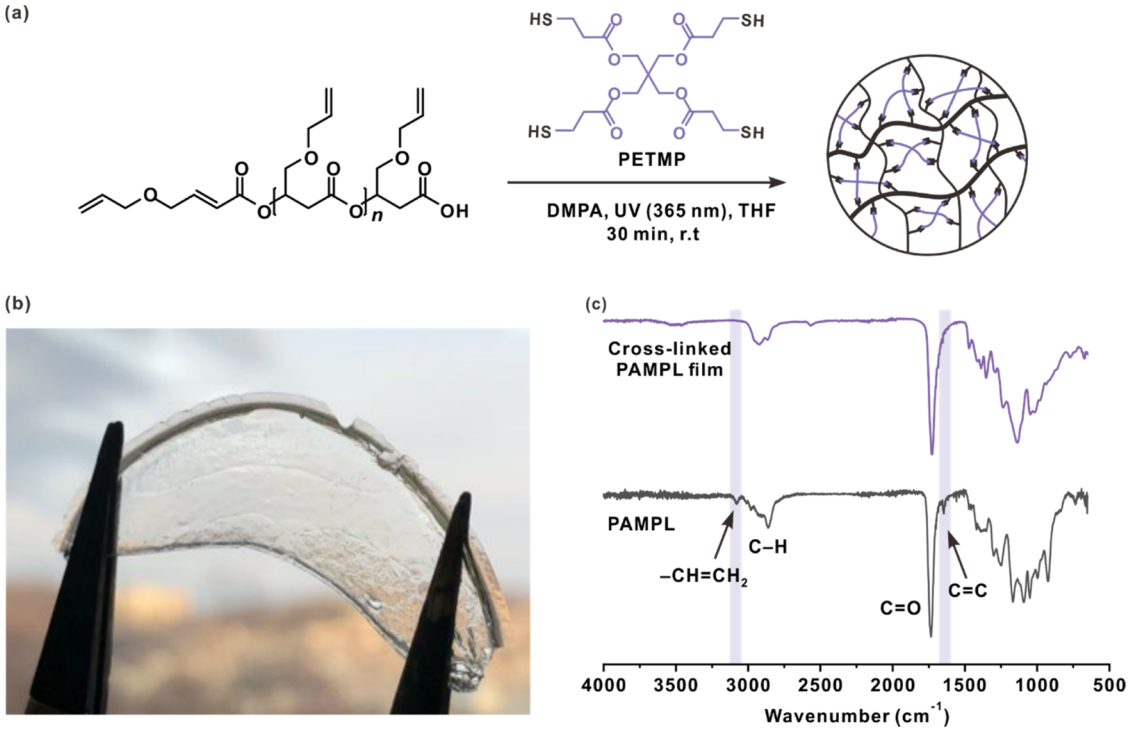

Figure 4. Characterization of cross-linked PAMPL film. (a) Thiol−ene reaction of PAMPL and PETMP with the DMPA photoinitiator, (b) photographic image of the PAMPL film cross-linked with PETMP, and (c) FTIR spectra of the resulting PAMPL polymer and the cross-linked film.

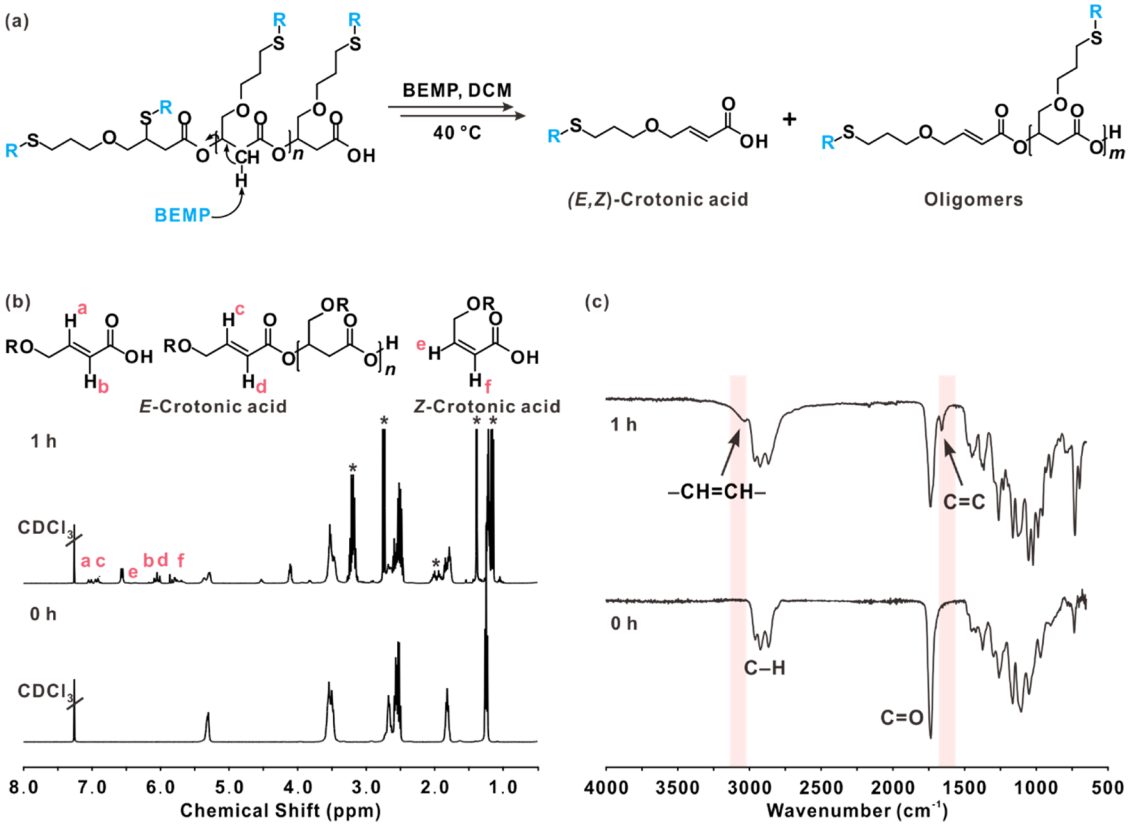

Figure 5. Chemical degradation of P_1. (a) Representative degradation mechanism mediated by BEMP with the (b) ^{1}H NMR and (c) FTIR spectra of P_1 and the degraded products. Note that BEMP is marked with an asterisk (*) in panel (b).

^{1}H NMR spectroscopy confirmed the complete conversion of the pendant allyl groups with the complete disappearance of the allyl group in the polymer side chain and the crotonate initiator peaks. New characteristic peaks corresponding to each

https://doi.org/10.1021/acs.macromol.1c01879
Macromolecules 2021, 54, 10903−10913

functional group were observed after the PPM of the PAMPL polymer; for example, all of the modified polymers of P_1−P_4 displayed the protons of the methylene groups adjacent to sulfur (2.50−2.89 ppm, j and a) along with the unique peaks from the respective thiol-based molecules, clearly evidencing the successful thiol−ene reaction (Figure 3b−e). It is worth noting that the solubility and thermal properties were significantly altered by the introduction of the different functional moieties. While PAMPL itself is soluble in polar aprotic solvents, the resulting ionic polymers (e.g., P_3 and P_4) were readily dissolved in polar protic solvents, such as water. Moreover, differential scanning calorimetry (DSC) studies provided the glass-transition temperatures (T_g) of the resulting polymers: −52.6 °C (P_1), −29.6 °C (P_2), −10.0 °C (P_3) and 47.1 °C (P_4) (Figure S18).

After the successful photoinitiated thiol−ene reaction of the PAMPL polymers was confirmed, PAMPL was subjected to photo-cross-linking using a PETMP cross linker to afford a cross-linked transparent PAMPL film (Figure 4a,b). FTIR spectroscopy showed that the characteristic peaks in PAMPL corresponding to methylene and methine (C−H stretching vibrations) and the C═O stretching vibrations of ester carbonyl in the polymer backbone were observed at 2918, 2854, and 1734 cm^{-1}, respectively, and the allyl (−CH═CH_2 stretching vibrations) and crotonate peaks (C═C stretching vibrations) were observed at 3083 and 1664 cm^{-1}, respectively. After the photo-cross-linking, the allyl and crotonate peaks disappeared, indicating the successful formation of the cross-linked PAMPL film (Figure 4c). The DSC thermogram of pure PAMPL showed a T_g of −42.5 °C, which increased significantly to −0.1 °C for a cross-linked film, indicating that the chain segment mobility is diminished upon cross-linking (Figure S19).

Furthermore, the mechanical properties of the cross-linked PAMPL film were evaluated using the universal testing machine. The stress−strain behavior of the cross-linked PAMPL film displayed a poor strain at break up of around 10% and a tensile strength of 0.25 MPa, which is likely due to the very low T_g (−42.5 °C) of the PMAPL backbone (Figure S20). Thus, the mechanical properties of this film need to be improved, and research on using other cross linkers with rigid moieties or embedding within a matrix is currently underway.

Degradation of the Functionalized PAMPL. The degradability of the prepared PAMPL polymers was examined under various conditions by subjecting the polymers to chemical, thermal, and biological degradations. First, using P_1 as a representative example, the functionalized PAMPL was chemically degraded by subjecting the polymer to a BEMP catalyst (15 equiv with respect to a functionalized PAMPL) dissolved in DCM at 40 °C. It should be noted here that BEMP does not degrade the polymer in the polymerization process as it only acts as a base in the initiation process; however, interestingly, it can be employed as a base for degrading polymers by homogeneously reacting with a polymer in excess. BEMP abstracts the α-proton in the backbone of the polymer, generating a crotonyl chain end via β-elimination (Figure 5a). The ^{1}H NMR spectra clearly indicated the appearance of the crotonic acids and oligomers end-capped with a crotonate within 1 h. The crotonate peak (6.01−6.10 and 6.87−7.06 ppm) reveals the formation of *E*-crotonic acid comprising 87% of the total degraded polymer, while the remainder corresponds to *Z*-crotonic acid (Figure 5b). FTIR analyses displayed the appearance of the characteristic crotonate peaks (−CH═CH− and C═C stretching vibrations) at 3080 and 1660 cm^{-1}, respectively (Figure 5c). In addition, the molecular weight measured via GPC clearly demonstrated the successful degradation of P_1 from 8200 to 830 g mol^{-1} (Figure S21). Similar degradation behaviors were observed for P_2 upon treatment with BEMP (Figures S22−S24).

We then further explored the thermal degradation of the P_1 polymer at 230 °C. A random polymer chain cleavage via β-elimination almost exclusively occurred in P_1 during thermal degradation, as similarly observed in PHB degradation.[51] ^{1}H NMR and FTIR spectroscopy confirmed the formation of crotonyl chain-end moieties and anhydride, which was formed by the condensation of two carboxylic acids, as evidenced by the increasing anhydride carbonyl stretching vibration at 1771 cm^{-1} (Figures S25 and S26). Furthermore, the GPC curves showed a gradual decrease of $M_{n,GPC}$ from 8200 to 1150 g mol^{-1} with a significant broadening of the molecular weight distribution from 1.17 to 4.50 after 5.5 h (Figure S27). After 24 h of thermal treatment, however, the P_1 polymer turned into a black solid that was insoluble in solvents.

Unlike the thermal degradation of P_1, the degradation product of P_2 did not dissolve in any solvent even after 1 h of thermal treatment, which limited further ^{1}H NMR and GPC characterizations. The FTIR spectra suggested similar degradation behaviors, as demonstrated by the increase of the crotonyl chain-end moiety and anhydride carbonyl peaks via chain cleavage due to β-elimination and the condensation of two carboxylic acid (Figure S28). Interestingly, the hydroxyl group peak at 3200−2600 cm^{-1} decreased, suggesting the transesterification of the alcohol moiety in the side chain and the ester in the P_2 polymer backbone (Figure S29). Note that the degradation of a polymer backbone can be controlled depending on the pendant groups attached to the side chain.

Degradation of the PAMPL Film. Next, to expand the utility of the synthesized PAMPL polymer in various conditions, the degradation behavior of the prepared film was analyzed. First, film degradation was performed in 0.10 M BEMP, 0.10 M NaOH, and 0.10 M HCl to chemically accelerate the degradation (Figure S30). By measuring the weight loss, the degradation rates under various chemical conditions were examined for 1 month. The cross-linked PAMPL film degraded as soon as it was placed in the 0.10 M BEMP solution. In contrast, the cross-linked PAMPL film degraded with a mass loss of 62 and 13% in 0.10 M NaOH and 0.10 M HCl, respectively, after incubation for 1 month. Although the basic condition facilitated the degradation of the polymers, the BEMP solution in DCM could more easily access the hydrophobic cross-linked PAMPL film compared to aqueous NaOH, which consequently significantly accelerated the degradation of the cross-linked polymer film.

Encouraged by the successful degradation of the polymer and cross-linked PAMPL film, we were prompted to extend the degradation in more environmentally accessible biological conditions (Figure 6). Therefore, laboratory biodegradation experiments were performed in composting soil and seawater to verify biodegradability in the natural environment. The cross-linked PAMPL films (500 μm in thickness) were placed in seawater and a compost and garden soil mixture (5:5, w/w) under either ambient conditions or incubated at 50 °C with the water content maintained at 50% (v/w). The biodegradation was monitored using gravimetric methods for 2 months. After 2 months, the films underwent degradation with

https://doi.org/10.1021/acs.macromol.1c01879
Macromolecules 2021, 54, 10903−10913

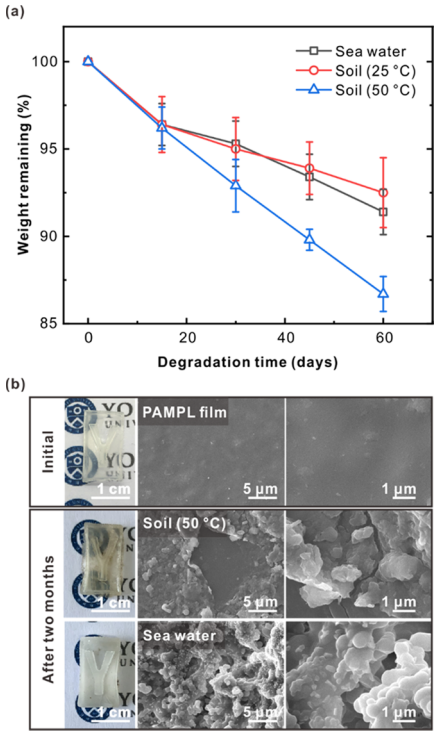

Figure 6. Degradation of the cross-linked PAMPL film under biological conditions. (a) Time-dependent weight loss of the cross-linked PAMPL film, and (b) (left) photographic images and (middle and right panel) SEM images of the initial and degraded films in the compost and garden soil mixture at 50 °C and seawater after 2 months. For each experiment, three films were used to report the average value with standard deviations.

a mass loss of 9, 7, and 14% in seawater, soil mixture under ambient conditions, and soil mixture at 50 °C, respectively (Figure 6a). Moreover, as estimated, the complete degradation of the films in a soil mixture at 50 °C would take approximately 453 days, assuming the zeroth-order kinetics for the degradation. For comparison, it has been previously demonstrated that the PHB films were degraded with 95% mass loss after 35 days in field soil at 28 °C with 50% moisture and 58% mass loss after 160 days in sea.[52,53]

The film degraded in the soil mixture at 50 °C showed slightly accelerated degradation rates compared to the films degraded in the soil mixture at ambient conditions and seawater, indicating the role of temperature in film degradation. Furthermore, the surface morphological changes of the degraded films were observed via SEM (Figure 6b). The films only exhibited color change without any noticeable damage. Interestingly, SEM observations indicated that the surfaces of the degraded films was rougher than the surfaces of the initial film and contained various pores. The morphology and distribution of the pores differed depending on the degradation condition. The difference in the rough surface morphology was probably due to the presence of different microorganisms in soil and seawater. Taking these results together, we conclude that the prepared PAMPL film can be biodegraded in natural environments.

CONCLUSIONS

In summary, we reported the design and synthesis of biodegradable PAMPL, a PHA derivative containing a pendant allyl group. The AMPL monomer was prepared via the carbonylation of allyl glycidyl ether, and subsequently, AROP was performed using various organocatalysts in bulk conditions. Particularly, BEMP was found to be the most suitable organocatalyst for producing PAMPL with a controllable molecular weight and dispersity without side reactions. The photoactivated thiol−ene reaction allowed the PPM of PAMPLs with varying substituents, influencing the solubility and the thermal properties of the functionalized PAMPL polymers. Furthermore, the degradability of the prepared PAMPL polymers was examined in chemical, thermal, and biological conditions. Most notably, the cross-linked PAMPL films were degraded in soil and seawater under a wide range of degradation kinetics. We anticipate that this study provides a facile approach for synthesizing and functionalizing PHA derivatives, presenting significant potential for future biodegradable plastics owing to their high biodegradability.

ASSOCIATED CONTENT

Supporting Information

The Supporting Information is available free of charge at https://pubs.acs.org/doi/10.1021/acs.macromol.1c01879.

Additional analysis including ^{1}H, ^{13}C, COSY, and HSQC NMR; FTIR; MALDI-TOF; GPC; DSC; and tensile stress−strain data (PDF)

AUTHOR INFORMATION

Corresponding Author

Byeong-Su Kim − *Department of Chemistry, Yonsei University, Seoul 03722, Republic of Korea;* orcid.org/0000-0002-6419-3054; Email: bskim19@yonsei.ac.kr

Authors

Yeji Yu − *Department of Chemistry, Yonsei University, Seoul 03722, Republic of Korea;* orcid.org/0000-0002-6880-6305

Minseong Kim − *Department of Chemistry, Yonsei University, Seoul 03722, Republic of Korea; Department of Chemistry, Ulsan National Institute of Science and Technology (UNIST), Ulsan 44919, Republic of Korea;* orcid.org/0000-0002-2612-922X

Gue Seon Lee − *Department of Chemistry and Research Institute of Physics and Chemistry, Jeonbuk National University, Jeonju 54896, Republic of Korea*

Hyo Won Lee − *Department of Chemistry and Research Institute of Physics and Chemistry, Jeonbuk National University, Jeonju 54896, Republic of Korea*

Jeung Gon Kim − *Department of Chemistry and Research Institute of Physics and Chemistry, Jeonbuk National University, Jeonju 54896, Republic of Korea*

Complete contact information is available at: https://pubs.acs.org/10.1021/acs.macromol.1c01879

Notes

The authors declare no competing financial interest.

ACKNOWLEDGMENTS

This work was supported by the National Research Foundation of Korea (NRF-2021R1A2C3004978).

REFERENCES

(1) Barnes, D. K. A.; Galgani, F.; Thompson, R. C.; Barlaz, M. Accumulation and Fragmentation of Plastic Debris in Global Environments. *Philos. Trans. R. Soc., B* **2009**, *364*, 1985−1998.

(2) Jambeck, J. R.; Geyer, R.; Wilcox, C.; Siegler, T. R.; Perryman, M.; Andrady, A.; Narayan, R.; Law, K. L. Plastic Waste Inputs from Land into the Ocean. *Science* **2015**, *347*, 768−771.

(3) Sheldon, R. A.; Norton, M. Green Chemistry and the Plastic Pollution Challenge: towards a Circular Economy. *Green Chem.* **2020**, *22*, 6310−6322.

(4) Gironi, F.; Piemonte, V. Bioplastics and Petroleum-based Plastics: Strengths and Weaknesses. *Energy Sources, Part A* **2011**, *33*, 1949−1959.

(5) Babu, R. P.; O'Connor, K.; Seeram, R. Current Progress on Bio-based Polymers and Their Future Trends. *Prog. Biomater.* **2013**, *2*, No. 8.

(6) Taniguchi, I.; Kagotani, K.; Kimura, Y. Microbial Production of Poly(hydroxyalkanoate)s from Waste Edible Oils. *Green Chem.* **2003**, *5*, 545−548.

(7) Chung, A.-L.; Jin, H.-L.; Huang, L.-J.; Ye, H.-M.; Chen, J.-C.; Wu, Q.; Chen, G.-Q. Biosynthesis and Characterization of Poly(3-hydroxydodecanoate) by β-Oxidation Inhibited Mutant of Pseudomonas Entomophila L48. *Biomacromolecules* **2011**, *12*, 3559−3566.

(8) Iwata, T. Biodegradable and Bio-based Polymers: Future Prospects of Eco-friendly Plastics. *Angew. Chem., Int. Ed.* **2015**, *54*, 3210−3215.

(9) Meereboer, K. W.; Misra, M.; Mohanty, A. K. Review of Recent Advances in the Biodegradability of Polyhydroxyalkanoate (PHA) Bioplastics and Their Composites. *Green Chem.* **2020**, *22*, 5519−5558.

(10) Thorat Gadgil, B. S.; Killi, N.; Rathna, G. V. N. Polyhydroxyalkanoates as Biomaterials. *MedChemComm* **2017**, *8*, 1774−1787.

(11) Tang, C.; Ryu, C. Y. Polyhydroxyalkanoates: Sustainability, Production, and Industrialization. In *Sustainable Polymers from Biomass*; Wiley-VCH Verlag GmbH & Co. KGaA, 2017; pp 11−33.

(12) Li, Y.; Strathmann, T. J. Kinetics and Mechanism for Hydrothermal Conversion of Polyhydroxybutyrate (PHB) for Wastewater Valorization. *Green Chem.* **2019**, *21*, 5586−5597.

(13) Shakaroun, R. M.; Jéhan, P.; Alaaeddine, A.; Carpentier, J.-F.; Guillaume, S. M. Organocatalyzed Ring-opening Polymerization (ROP) of Functional β-Lactones: New Insights into the ROP Mechanism and Poly(hydroxyalkanoate)s (PHAs) Macromolecular structure. *Polym. Chem.* **2020**, *11*, 2640−2652.

(14) Vroman, I.; Tighzert, L. Biodegradable Polymers. *Materials* **2009**, *2*, 307−344.

(15) Allmendinger, M.; Eberhardt, R.; Luinstra, G.; Rieger, B. The Cobalt-Catalyzed Alternating Copolymerization of Epoxides and Carbon Monoxide: A Novel Approach to Polyesters. *J. Am. Chem. Soc.* **2002**, *124*, 5646−5647.

(16) Allmendinger, M.; Eberhardt, R.; Luinstra, G. A.; Rieger, B. Alternating Copolymerization Reaction of Propylene Oxide and CO: Variation of Polymer Stereoregularity and Investigation into Chain Termination. *Macromol. Chem. Phys.* **2003**, *204*, 564−569.

(17) Lee, J. T.; Alper, H. Alternating Copolymerization of Propylene Oxide and Carbon Monoxide to form Aliphatic Polyesters. *Macromolecules* **2004**, *37*, 2417−2421.

(18) Coulembier, O.; Degée, P.; Hedrick, J. L.; Dubois, P. From Controlled Ring-Opening Polymerization to Biodegradable Aliphatic Polyester: Especially Poly(β-malic acid) Derivatives. *Prog. Polym. Sci.* **2006**, *31*, 723−747.

(19) Bandelli, D.; Alex, J.; Weber, C.; Schubert, U. S. Polyester Stereocomplexes Beyond P. L. A.:. Could Synthetic Opportunities Revolutionize Established Material Blending? *Macromol. Rapid Commun.* **2020**, *41*, No. 1900560.

(20) Gabirondo, E.; Sangroniz, A.; Etxeberria, A.; Torres-Giner, S.; Sardon, H. Poly(hydroxy acids) Derived from the Self-Condensation of Hydroxy Acids: from Polymerization to End-of-Life Options. *Polym. Chem.* **2020**, *11*, 4861−4874.

(21) Rieth, L. R.; Moore, D. R.; Lobkovsky, E. B.; Coates, G. W. Single-Site β-Diiminate Zinc Catalysts for the Ring-Opening Polymerization of β-Butyrolactone and β-Valerolactone to Poly(3-hydroxyalkanoates). *J. Am. Chem. Soc.* **2002**, *124*, 15239−15248.

(22) Li, Y.-T.; Yu, H.-Y.; Li, W.-B.; Liu, Y.; Lu, X.-B. Recyclable Polyhydroxyalkanoates via a Regioselective Ring-Opening Polymerization of α,β-Disubstituted β-Lactone Monomers. *Macromolecules* **2021**, *54*, 4641−4648.

(23) Dijkstra, P. J.; Du, H.; Feijen, J. Single Site Catalysts for Stereoselective Ring-Opening Polymerization of Lactides. *Polym. Chem.* **2011**, *2*, 520−527.

(24) Thomas, C. M. Stereocontrolled Ring-Opening Polymerization of Cyclic Esters: Synthesis of New Polyester Microstructures. *Chem. Soc. Rev.* **2010**, *39*, 165−173.

(25) Carpentier, J.-F. Discrete Metal Catalysts for Stereoselective Ring-Opening Polymerization of Chiral Racemic β-Lactones. *Macromol. Rapid Commun.* **2010**, *31*, 1696−1705.

(26) Kramer, J. W.; Treitler, D. S.; Dunn, E. W.; Castro, P. M.; Roisnel, T.; Thomas, C. M.; Coates, G. W. Polymerization of Enantiopure Monomers Using Syndiospecific Catalysts: A New Approach To Sequence Control in Polymer Synthesis. *J. Am. Chem. Soc.* **2009**, *131*, 16042−16044.

(27) Carpentier, J.-F. Exploitation of a Chain-End-Control Mechanism for the Synthesis of Alternating Copolymers. *Angew. Chem., Int. Ed.* **2010**, *49*, 2662−2663.

(28) Jaffredo, C. G.; Carpentier, J.-F.; Guillaume, S. M. Controlled ROP of β-Butyrolactone Simply Mediated by Amidine, Guanidine, and Phosphazene Organocatalysts. *Macromol. Rapid Commun.* **2012**, *33*, 1938−1944.

(29) Kiesewetter, M. K.; Shin, E. J.; Hedrick, J. L.; Waymouth, R. M. Organocatalysis: Opportunities and Challenges for Polymer Synthesis. *Macromolecules* **2010**, *43*, 2093−2107.

(30) Du, F.; Zheng, Y.; Yuan, W.; Shan, G.; Bao, Y.; Jie, S.; Pan, P. Solvent-Free Ring-Opening Polymerization of Lactones with Hydrogen-Bonding Bisurea Catalyst. *J. Polym. Sci., Part A: Polym. Chem.* **2019**, *57*, 90−100.

(31) García-Valle, F. M.; Tabernero, V.; Cuenca, T.; Mosquera, M. E. G.; Cano, J.; Milione, S. Biodegradable PHB from rac-β-Butyrolactone: Highly Controlled ROP Mediated by a Pentacoordinated Aluminum Complex. *Organometallics* **2018**, *37*, 837−840.

(32) Guillaume, S. M.; Annunziata, L.; Rosal, I. D.; Iftner, C.; Maron, L.; Roesky, P. W.; Schmid, M. Ring-Opening Polymerization of Racemic β-Butyrolactone Promoted by Rare Earth Trisborohydride Complexes towards a PHB-Diol: an Experimental and DFT Study. *Polym. Chem.* **2013**, *4*, 3077−3087.

(33) Yang, L.; Zhang, Y.-Y.; Yang, G.-W.; Xie, R.; Wu, G.-P. Controlled Ring-Opening Polymerization of β-Butyrolactone Via Bifunctional Organoboron Catalysts. *Macromolecules* **2021**, *54*, 5509−5517.

(34) Rastogi, V.; Samyn, P. Bio-Based Coatings for Paper Applications. *Coatings* **2015**, *5*, 887−930.

(35) Smith, M. K. M.; Paleri, D. M.; Abdelwahab, M.; Mielewski, D. F.; Misra, M.; Mohanty, A. K. Sustainable Composites from Poly(3-hydroxybutyrate) (PHB) Bioplastic and Agave Natural Fibre. *Green Chem.* **2020**, *22*, 3906−3916.

(36) Wilson, J. E.; Fu, G. C. Asymmetric Synthesis of Highly Substituted β-Lactones by Nucleophile-Catalyzed [2+2] Cycloadditions of Disubstituted Ketenes with Aldehydes. *Angew. Chem.* **2004**, *116*, 6518−6520.

(37) Smith, N. D.; Wohlrab, A. M.; Goodman, M. Enantiocontrolled Synthesis of α-Methyl Amino Acids via Bn2N-α-Methylserine-β-lactone. *Org. Lett.* **2005**, *7*, 255−258.

(38) Baral, E. R.; Kim, D.; Lee, S.; Park, M. H.; Kim, J. G. Tin(IV)-Porphyrin Tetracarbonyl Cobaltate: An Efficient Catalyst for the Carbonylation of Epoxides. *Catalysts* **2019**, *9*, No. 311.

(39) Lee, J. T.; Thomas, P. J.; Alper, H. Synthesis of β-Lactones by the Regioselective, Cobalt and Lewis Acid Catalyzed Carbonylation of Simple and Functionalized Epoxides. *J. Org. Chem.* **2001**, *66*, 5424−5426.

https://doi.org/10.1021/acs.macromol.1c01879
Macromolecules 2021, 54, 10903−10913

(40) Schmidt, J. A. R.; Lobkovsky, E. B.; Coates, G. W. Chromium(III) Octaethylporphyrinato Tetracarbonylcobaltate: A Highly Active, Selective, and Versatile Catalyst for Epoxide Carbonylation. *J. Am. Chem. Soc.* **2005**, *127*, 11426−11435.
(41) Kramer, J. W.; Lobkovsky, E. B.; Coates, G. W. Practical β-Lactone Synthesis: Epoxide Carbonylation at 1 atm. *Org. Lett.* **2006**, *8*, 3709−3712.
(42) Obermeier, B.; Frey, H. Poly(ethylene glycol-co-allyl glycidyl ether)s: A PEG-Based Modular Synthetic Platform for Multiple Bioconjugation. *Bioconjugate Chem.* **2011**, *22*, 436−444.
(43) Blasco, E.; Sims, M. B.; Goldmann, A. S.; Sumerlin, B. S.; Barner-Kowollik, C. 50th Anniversary Perspective: Polymer Functionalization. *Macromolecules* **2017**, *50*, 5215−5252.
(44) Sathyan, A.; Hayward, R. C.; Emrick, T. Ring-Opening Polymerization of Allyl-Functionalized Lactams. *Macromolecules* **2019**, *52*, 167−175.
(45) Zhang, X.; Li, Z.; Che, X.; Yu, L.; Jia, W.; Shen, R.; Chen, J.; Ma, Y.; Chen, G.-Q. Synthesis and Characterization of Polyhydroxyalkanoate Organo/Hydrogels. *Biomacromolecules* **2019**, *20*, 3303−3312.
(46) Zhao, Z.; Shen, Y.; Kou, X.; Shi, J.; Wang, R.; Liu, F.; Li, Z. Organocatalytic Ring-Opening Copolymerization of Biorenewable α-Methylene-γ-Butyrolactone toward Functional Copolyesters: Preparation and Composition Dependent Thermal Properties. *Macromolecules* **2020**, *53*, 3380−3389.
(47) Mattson, K. M.; Latimer, A. A.; McGrath, A. J.; Lynd, N. A.; Lundberg, P.; Hudson, Z. M.; Hawker, C. J. A Facile Synthesis of Catechol-Functionalized Poly(ethylene oxide) Block and Random Copolymers. *J. Polym. Sci., Part A: Polym. Chem.* **2015**, *53*, 2685−2692.
(48) Kim, H.; Jeon, H.; Shin, G.; Lee, M.; Jegal, J.; Hwang, S. Y.; Oh, D. X.; Koo, J. M.; Eom, Y.; Park, J. Biodegradable Nanocomposite of Poly(ester-co-carbonate) and Cellulose Nanocrystals for Tough Tear-Resistant Disposable Bags. *Green Chem.* **2021**, *23*, 2293−2299.
(49) Sui, H.; Zhou, J.; Ma, G.; Niu, Y.; Cheng, J.; He, L.; Li, X. Removal of Ionic Liquids from Oil Sands Processing Solution by Ion-Exchange Resin. *Appl. Sci.* **2018**, *8*, No. 1611.
(50) Domiński, A.; Konieczny, T.; Zięba, M.; Klim, M.; Kurcok, P. Anionic Polymerization of β-Butyrolactone Initiated with Sodium Phenoxides. The Effect of the Initiator Basicity/Nucleophilicity on the ROP Mechanism. *Polymers* **2019**, *11*, No. 1221.
(51) Wang, S.; Chen, W.; Xiang, H.; Yang, J.; Zhou, Z.; Zhu, M. Modification and Potential Application of Short-Chain-Length Polyhydroxyalkanoate (SCL-PHA). *Polymers* **2016**, *8*, No. 273.
(52) Woolnough, C. A.; Yee, L. H.; Charlton, T. S.; Foster, L. J. R. A Tuneable Switch for Controlling Environmental Degradation of Bioplastics: Addition of Isothiazolinone to Polyhydroxyalkanoates. *PLoS One* **2013**, *8*, No. e75817.
(53) Volova, T. G.; Prudnikova, S. V.; Vinogradova, O. N.; Syrvacheva, D. A.; Shishatskaya, E. I. Microbial Degradation of Polyhydroxyalkanoates with Different Chemical Compositions and Their Biodegradability. *Microb. Ecol.* **2017**, *73*, 353−367.

https://doi.org/10.1021/acs.macromol.1c01879
Macromolecules 2021, 54, 10903−10913